ARTICLE

Immunohistochemical Localization of α-Smooth Muscle Actin During Rat Molar Tooth Development

Akihiro Hosoya, Hiroaki Nakamura, Tadashi Ninomiya, Kunihiko Yoshiba, Nagako Yoshiba, Hiroyuki Nakaya, Shigeyuki Wakitani, Hirohito Yamada, Etsuo Kasahara, and Hidehiro Ozawa

Department of Oral Histology (AH,HNakamura), Institute for Dental Science (TN,HO), and Department of Endodontics and Operative Dentistry (HY,EK), Matsumoto Dental University, Shiojiri, Nagano, Japan; Division of Cariology, Department of Oral Health Science, Course for Oral Life Science, Niigata University Graduate School of Medical and Dental Sciences, Niigata, Japan (KY,NY); and Department of Orthopedic Surgery, Shinshu University Graduate School of Medicine, Matsumoto, Nagano, Japan (HNakaya,SW)

SUMMARY   The dental follicle contains mesenchymal cells that differentiate into osteoblasts, cementoblasts, and fibroblasts. However, the characteristics of these mesenchymal cells are still unknown. α-Smooth muscle actin (α-SMA) is known to localize in stem cells and precursor cells of various tissues. In the present study, to characterize the undifferentiated cells in the dental follicle, immunohistochemical localization of α-SMA was examined during rat molar tooth development. Rat mandibles were collected at embryonic days (E) 15–20 and postnatal days (P) 7–28. Immunohistochemical stainings for α-SMA, periostin, Runt-related transcription factor-2 (Runx2), tissue nonspecific alkaline phosphatase (TNAP), and bone sialoprotein (BSP) were carried out using paraffin-embedded sections. α-SMA localization was hardly detected in the bud and cap stages. At the early bell stage, α-SMA-positive cells were visible in the dental follicle around the cervical loop. At the late bell to early root formation stage (P14), these cells were detected throughout the dental follicle, but they were confined to the apical root area at P28. Double immunostaining for α-SMA and periostin demonstrated that α-SMA-positive cells localized to the outer side of periostin-positive area. Runx2-positive cells were visible in the α-SMA-positive region. TNAP-positive cells in the dental follicle localized nearer to alveolar bone than Runx2-positive cells. BSP was detected in osteoblasts as well as in alveolar bone matrix. These results demonstrate that α-SMA-positive cells localize on the alveolar bone side of the dental follicle and may play a role in alveolar bone formation.
     (J Histochem Cytochem 54:1371–1378, 2006)

THE DENTAL FOLLICLE surrounding the tooth germ contains mesenchymal cells that are able to differentiate into osteoblasts, cementoblasts, and fibroblasts (Nanci 2003). As a result, this tissue is able to form the periodontal tissues including alveolar bone, cementum, and periodontal ligament. However, the characteristics and distribution of undifferentiated cells within the dental follicle and periodontal tissues are still unclear.

Previous reports have described α-smooth muscle actin (α-SMA) as a cytoskeletal protein that is localized

to some stem and precursor cells (Cai et al. 2001; Kinner et al. 2002; Yamada et al. 2005). This protein has also been found in various tissues during tissue repair and regeneration following injury (Chaponnier and Gabbiani 2004; van Beurden et al. 2005). Thus, α-SMA may be a suitable marker of undifferentiated cells (Kinner et al. 2002). Additionally, in mature tissues, α-SMA is localized to pericytes of blood vessels, intestinal muscularis mucosae, and myoepithelial cells of mammary and salivary glands (Mukai et al. 1981; Skalli et al. 1986), which are required in a force-generating capacity. However, the temporospatial localization of α-SMA in developing and mature teeth has not been previously examined.

On the other hand, regeneration of periodontal tissues, lost as a result of periodontal disease, is a key

objective of periodontal treatment. Several surgical techniques have been developed to assist with regeneration of periodontal tissues including guided tissue regeneration, bone grafting, and the use of enamel matrix derivative (Emdogain; Straumann, Basel, Switzerland), but their success is not predictable. Development of new periodontal regeneration therapies using the undifferentiated cells in the periodontal tissues thus remains ongoing. The human periodontal ligament contains multipotent stem cells that differentiate into osteoblasts, cementoblasts, and fibroblasts, and these cells could possibly be used to induce periodontal regeneration (Seo et al. 2004,2005). Additionally, the dental follicle has been utilized as a source of undifferentiated cells in in vitro and in vivo studies (Saito et al. 2005). Because the dental follicle and periodontal ligament are immunopositive for periostin (Kruzynska-Frejtag et al. 2004; Suzuki et al. 2004), this protein is often used as a marker of these tissues. However, determining the degree of cell differentiation could not be readily ascertained. A more definitive understanding of the periodontal tissue could assist with the development of regenerative methods using periodontal cells.

The differentiation process of alveolar bone-formative osteoblasts has also not been clarified. Bone morphogenetic proteins (BMPs) and/or transforming growth factor (TGF)-β act on undifferentiated cells and phosphorylate R-Smads through their receptors. These phosphorylated R-Smads subsequently interact with Smad4 and translocate to the nucleus (Derynck et al. 1998; Shi and Massague 2003). Thereafter, Runx2, the essential transcription factor for osteoblast differentiation, is expressed in osteogenic cells and induces the expression of bone matrix proteins such as osteopontin (OPN) and bone sialoprotein (BSP) (Lian et al. 2004). In these processes, expression of tissue nonspecific alkaline phosphatase (TNAP) is also increased (Hoshi et al. 1997; Hosoya et al. 2003).

In the present study, we show that α-SMA is specifically expressed in the dental follicle. In addition, to examine the distribution pattern of α-SMA and the differentiation process of these positive cells, immunohistochemical localization of α-SMA and other differentiation marker proteins were examined during rat molar tooth development. The marker of the dental follicle used was periostin-specific antibody. Observations of cell differentiation process in α-SMA-positive area were also undertaken and involved the use of Smad4-, Runx2-, OPN-, BSP-, and TNAP-specific antibodies.

Materials and Methods

All experiments were performed according to guidelines set forth by the Matsumoto Dental University Committee on Intramural Animal Use.

Western Blotting

First molar tooth germs of E15, 17, and 20 Wistar rats were removed from the mandible. Samples were dissolved in 100 μl of sample buffer containing 4% SDS, 20% glycerol, and 12% mercaptoethanol in 100 mM Tris–HCl (pH 6.8) and heated at 100C for 5 min. These lysates were quantified by BCA protein assay kit (Pierce Biotechnology; Rockford, IL), and an equal amount (30 μg) of each lysate was fractionated by SDS-PAGE using 12% polyacrylamide gel. Samples were then electrophoresed at 150 V for 60 min and transferred to a nitrocellulose membrane using 192 mM glycine and 20% methanol in 25 mM Tris–HCl (pH 8.3) at a constant amperage of 50 mA for 60 min. The membrane was immersed in 10 mM TBS, pH 7.4, containing 10% skim milk for 30 min to block nonspecific binding. It was subsequently incubated with mouse monoclonal antibody against human α-SMA (1A4;R&D Systems, Minneapolis, MN), diluted 1:1000 for 12 hr at 4C, and then with horseradish peroxidase (HRP)-conjugated anti-mouse IgG (Sigma; St Louis, MO) for 1 hr at room temperature. Immunoreactivity was visualized using ECL Western blotting detection reagents (Amersham Pharmacia Biotech UK Ltd.; Buckinghamshire, England) according to the manufacturer's instructions. The membrane was then reprobed in 2% SDS, 62.5 mM Tris–HCl (pH 6.7), and 100 mM 2-mercaptoethanol for 30 min at 50C and subsequently incubated with rabbit anti-mouse actin polyclonal antibody (Biomedical Technologies; Stoughton, MA), and HRP-conjugated anti-rabbit IgG (Sigma) for comparison of the amount of total protein.

Immunohistochemistry

Rat mandibles were collected at E15–20 and P7–28 and fixed with 4% paraformaldehyde in 0.1 M phosphate buffer (pH 7.4) for 24 hr at 4C. After demineralization with 10% EDTA, pH 7.4, for 3 weeks at 4C, the specimens were embedded in paraffin and sectioned at a thickness of 4 μm. Sections were then treated with 0.3% H_2O_2 in PBS, pH 7.4, for 30 min at room temperature to inactivate endogenous peroxidase. They were pretreated with 10% BSA (Seikagaku; Tokyo, Japan) in PBS for 1 hr at room temperature and incubated in mouse monoclonal antibodies against human α-SMA, human Smad4 (Santa Cruz Biotechnology; Santa Cruz, CA), and rabbit polyclonal antibodies against mouse Runx2 (Santa Cruz Biotechnology), rat TNAP (provided by Dr. Y. Ikehara), mouse OPN (provided by Dr. M. Fukae), human BSP (LF-120, provided by Dr. L.W. Fisher) for 12 hr at 4C. The antibodies against α-SMA, TNAP, OPN, and BSP were diluted to 1:500, and Smad4 and Runx2 antibodies were diluted to 1:100. Sections were reacted with Histofine Simple Stain rat MAX-PO (MULTI; Nichirei Co., Tokyo, Japan) for 1 hr at room temperature. Immune complexes were visualized using DAB (Envision kit; DAKO, Carpinteria, CA). Immunostained sections were then counterstained with hematoxylin. Non-immune mouse or rabbit sera were diluted to the same strength for use as negative controls. Control sections did not show any specific immunoreactivity.

Double-immunofluorescence staining was performed using mouse monoclonal antibody against human α-SMA and rabbit polyclonal antibody against human periostin (Bio-Vendor Laboratory; Heidelberg, Germany). Sections were pretreated with 10% BSA in PBS for 1 hr at room temperature

and incubated with 1:100 diluted primary antibodies for 12 hr at 4C. Sections were then incubated with 1:100 diluted Alexa-Fluor-488-conjugated anti-mouse IgG (Molecular Probes; Eugene, OR) and Alexa-Fluor-594-conjugated anti rabbit IgG (Molecular Probes) as secondary antibodies for 1 hr at room temperature. Samples were evaluated using a fluorescent microscope (Axioplan 2; Carl Zeiss, Jena, Germany) with the appropriate filter combinations.

Results

Localization of α-SMA During the Bud, Cap, and Early Bell Stages of Tooth Development

Western blotting analysis revealed that α-SMA antibody did not react with the lysate of E15 mandibular molar tooth germ. However, this antibody did react with the lysate of E17 and E20 tooth germs, with the intensity of reactivity increasing as tooth development progressed (Figure 1A).

Immunohistochemical localization of α-SMA was scarce in the tooth germ at the bud (E15) and cap (E17) stages (Figures 1B and 1C). At the early bell stage (E20), the dental follicle around the cervical loop displayed α-SMA immunoreactivity (Figures 1D and 1E). This immunoreactivity was seen within the cytoplasm of dental follicle cells possessing long cell processes (Figure 1F). The enamel organ and dental papillae showed no immunoreactivity.

Localization of α-SMA During the Late Bell and Root Formation Stages of Tooth Development

At the late bell stage (P7), α-SMA-positive cells were seen in the dental follicle surrounding the enamel organ
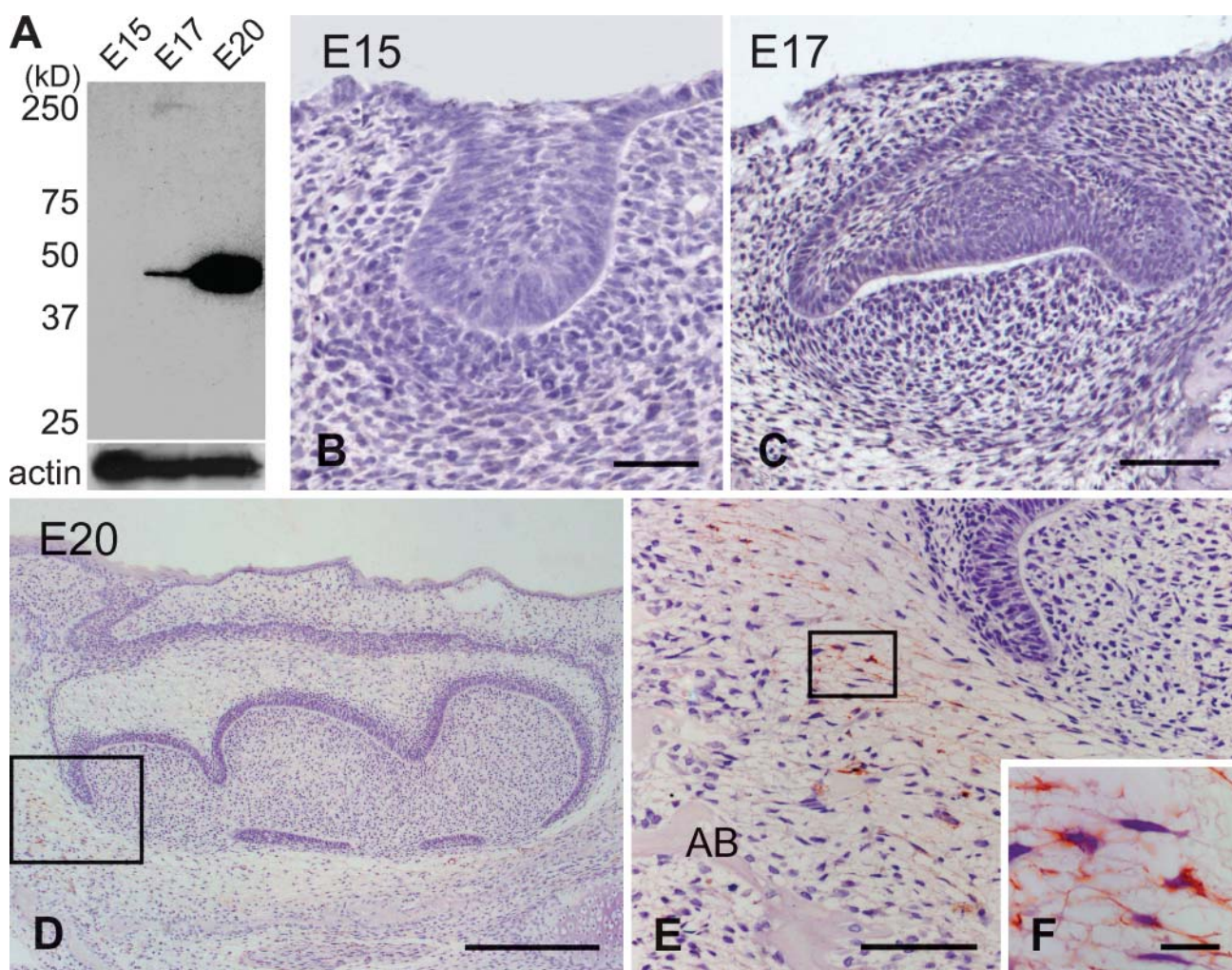

Figure 1 Western blotting analysis (**A**) and immunohistochemical staining of α-smooth muscle actin (αSMA) in the mandibular first molar at E15 (**B**), E17 (**C**), and E20 (**D–F**). Higher magnification of the boxed regions in **D** and **E** are shown in **E** and **F**, respectively. (**A**) α-SMA antibody reacted with cells in the E17 and E20 tooth germ. (**B,C**) α-SMA-positive cells are scarce in the tooth germs at the bud and cap stages. (**D,E**) The dental follicle cells around the cervical loop show α-SMA immunoreactivity at the early bell stage. (**F**) These cells exhibit long cell processes. AB, alveolar bone. Bars: **B,E** = 60 μm; **C** = 100 μm; **D** = 300 μm; **F** = 10 μm.

(Figure 2A). These cells seemed to localize on the alveolar bone side of the dental follicle (Figures 2B and 2C). Pericytes and smooth muscle cells of blood vessels surrounding the tooth germ and within the bone marrow displayed immunoreactivity. The surface of the alveolar bone, except the surface adjacent to the tooth germ, showed no immunoreactivity (Figure 2A). At the root formation stage (P14), intense immunostaining for α-SMA was observed in the dental follicle around Hertwig's epithelial root sheath (HRS). The dental follicle surrounding the enamel organ showed weaker immunoreactivity than that around HRS (Figures 2D–2F). As root formation progressed (P28), α-SMA-positive cells were confined to the apical region of the dental follicle

(Figures 3A and 3C). In the upper region of the periodontal space, there was no immunoreactivity for α-SMA, except for that associated with the blood vessels (Figure 3B). In the pulp tissue, pericytes and smooth muscle cells of the blood vessels were positive for α-SMA, but odontoblasts and pulp cells showed no immunoreactivity (Figure 3A).

α-SMA and Periostin Localization in the Dental Follicle

In the root apex of P28, α-SMA-positive cells were localized to the dental follicle. Pericytes and smooth muscle cells of the blood vessels in the periodontal space were also immunopositive for α-SMA (Figure 4A). Periostin was localized to the apical region of the dental follicle and
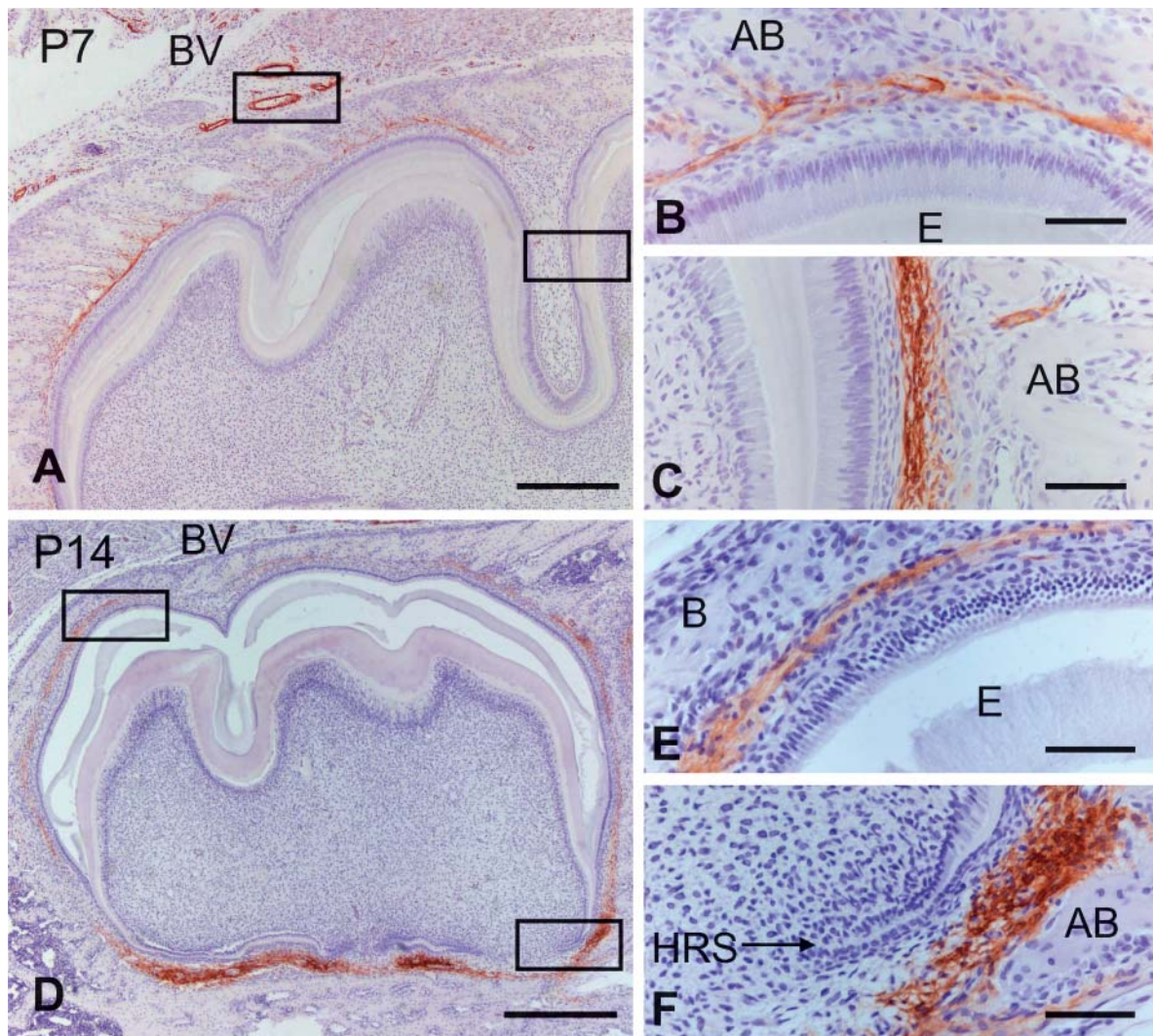

Figure 2 Immunohistochemical staining of α-SMA in the mandibular first molar at P7 (**A–C**) and P14 (**D–F**). Higher magnification of the boxed regions in **A** and **D** are shown in **B** and **C** and **E** and **F**, respectively. (**A**) α-SMA immunoreactivity is localized to the dental follicle surrounding the tooth crown at the late bell stage. (**B,C**) α-SMA-positive cells are visible on the alveolar bone (AB) side of the dental follicle. (**D–F**) Intense immunostaining for α-SMA is detected in the dental follicle along Hertwig's epithelial root sheath (HRS), whereas the dental follicle surrounding the tooth crown shows less immunoreactivity. BV, blood vessel; E, enamel. Bars: **A,D** = 600 μm; **B,C,E,F** = 100 μm.
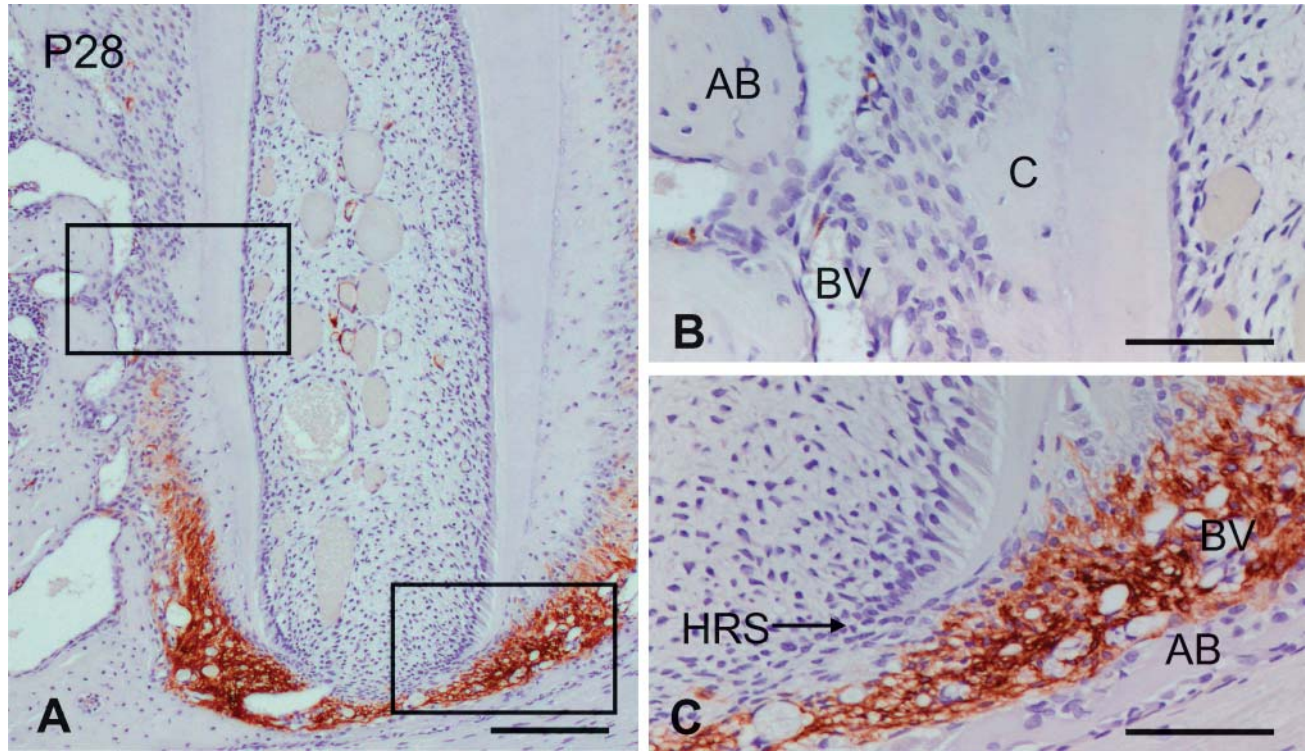
Figure 3 Immunohistochemical staining of α-SMA in the mandibular first molar at P28. Higher magnifications of the boxed regions in **A** are shown in **B** and **C**. **(A)** α-SMA immunoreactivity is apparent in the apical region dental follicle. **(B)** α-SMA immunoreactivity is not visible in osteoblasts, cementoblasts, and fibroblasts. **(C)** Intense immunostaining for α-SMA is seen in the dental follicle near HRS. AB, alveolar bone; BV, blood vessel; C, cementum. Bars: **A** = 150 μm; **B,C** = 40 μm.

to the periodontal ligament (Figure 4B). The merged image demonstrated that α-SMA-positive cells localized on the outer side of the dental follicle showing periostin immunoreactivity (Figure 4C). This staining pattern of α-SMA and periostin in whole regions of the dental follicle was consistent from E20 to P14 (not shown).

Distribution of Osteoblast Differentiation Marker Proteins in the Root Apex

In the root apex at P28, Smad4- and Runx2-positive cells were distributed in the apical dental follicle consistent with α-SMA-positive region (Figures 5A and 5B). TNAP-positive cells in the dental follicle localized closer to alveolar bone than Smad4- and Runx2-positive cells (Figure 5C). Immunostaining for OPN and BSP was detected in osteoblasts, as well as in alveolar bone matrix (Figures 5D and 5E).

Discussion

In the present study, α-SMA-positive cells were detected on the outer side of a periostin-positive area, and a relationship between α-SMA and periostin was observed during all stages of tooth development. Periostin is a protein specifically localized to the dental follicle and periodontal ligament (Kruzynska-Frejtag et al. 2004;

Suzuki et al. 2004), suggesting that α-SMA-positive cells localize on the alveolar bone side of the dental follicle but not in the dental follicle near the outer enamel epithelium. This finding seems to confirm the idea that the dental follicle does not contain a homogeneous cell population and is divided into two regions (Schroeder 1991). In addition, because α-SMA-positive cells were localized on the alveolar bone side of the dental follicle, these cells are presumed to be involved in alveolar bone formation. This is supported by a previous study showing that MC3T3-E1, an osteoblast-like cell line, synthesizes α-SMA during the undifferentiated stage (Menard et al. 2000). Furthermore, because BMPs, especially BMP3, are expressed in some dental follicle cells, it is thought that BMPs regulate the formation of the osteoblast during root formation (Yamashiro et al. 2003). In the present study we determined the immunohistochemical localization of osteoblast differentiation marker proteins Smad4, Runx2, TNAP, OPN, and BSP, which are known to be downstream proteins of BMPs, in α-SMA-positive regions. Smad4- and/or Runx2-positive cells were detected in α-SMA-positive areas. In addition, TNAP-, OPN-, and BSP-positive cells were detected closer to the alveolar bone, suggesting that α-SMA-positive cells may differentiate into osteoblasts.
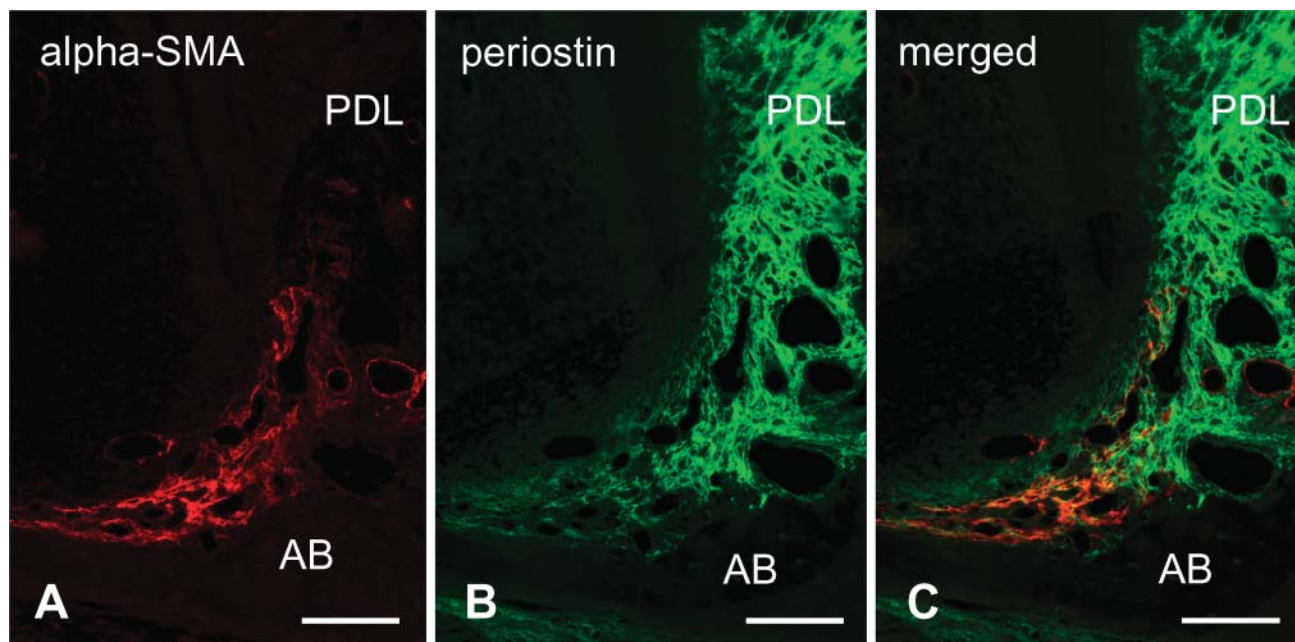
Figure 4 Double-immunofluorescence staining of α-SMA (shown in red) and periostin (in green) in the apical root at P28. **(A)** α-SMA localization is seen in the dental follicle at the root apex. **(B)** Periostin is localized to the dental follicle and periodontal ligament (PDL). **(C)** The area of α-SMA immunopositivity exists on the alveolar bone (AB) side of the periostin-positive area. Bar = 100 μm.

The areas of ectomesenchyme in bud (E15) and cap (E17) stages are believed to be undifferentiated. However, they were immunonegative for α-SMA. On the other hand, some dental follicle cells after early bell stage showed immunopositivity, suggesting that α-SMA begins to be expressed into some undifferentiated cells when they embark upon their differentiation process in the dental follicle. In addition, α-SMA-positive cells disappeared in the upper region of the periodontal tissues as root formation progressed (P28). Therefore, α-SMA may be a useful marker for determining the degree of cell differentiation in the dental follicle and in periodontal tissues.

The function of α-SMA is not clearly understood. α-SMA-expressing dental pulp cells increased with time in culture, and these cells have the contractile capacity to collagen–glycosaminoglycan analog of extracellular matrix in vitro (Brock et al. 2002). In addition, α-SMA is highly expressed in vascular smooth muscle cells, suggesting that it is required in a force-generating capacity. However, α-SMA null mice appear to have no abnormality in vascular contractility and blood pressure homeostasis, as a result of the partial substitution with other actin isoforms (Schildmeyer et al. 2000). It is thought that the dental follicle and periodontal ligament are implicated in the process of tooth eruption, and tooth eruption is linked to the contractility of fibroblasts. In the present study, α-SMA-positive region was shifted from the pericoronal dental follicle to the apical root at the beginning of root formation (P14) and con-

fined to the apical root area by the late root formation stage (P28). Furthermore, although the number of α-SMA-positive cells decreased over time, the localization pattern in the apical root area was similar in 1-year-old rats (not shown). Therefore, expression of α-SMA may play a possible role in cell contractile capacity and tooth eruption. Meanwhile, α-SMA is also thought to act in the maintenance of the undifferentiated cell in an angiogenic capacity (Kinner et al. 2002; Hinz et al. 2003; Chaponnier and Gabbiani 2004). Further research into the role of α-SMA in tooth formation is required.

In conclusion, α-SMA is localized to the alveolar bone side of the dental follicle cells after the bell stage of tooth formation. This suggests that these cells might differentiate into osteoblasts and contribute to alveolar bone formation. Our results also suggest that α-SMA might be a useful marker of undifferentiated dental follicle cells for research into periodontal development and regeneration.
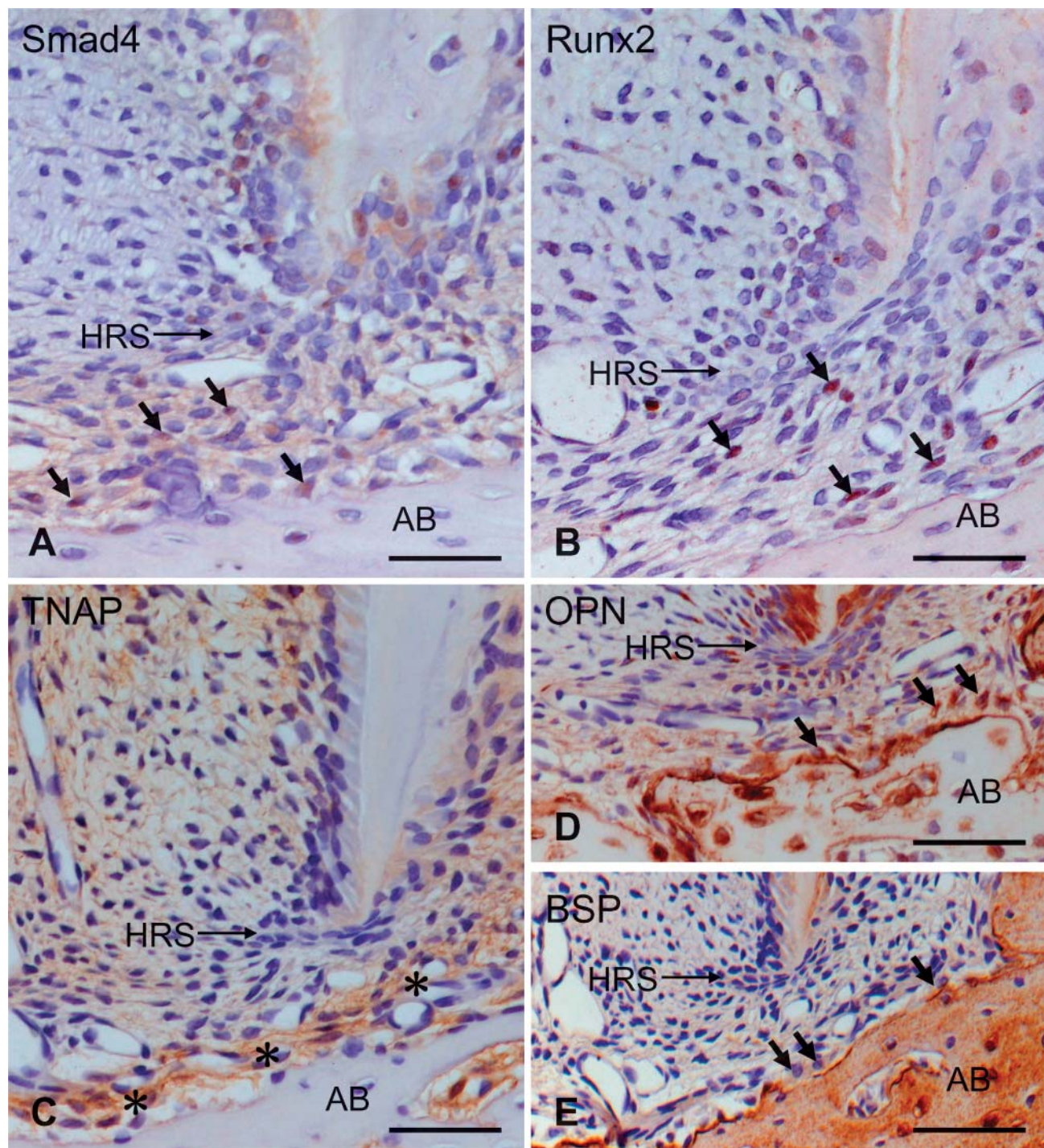
Figure 5 Immunohistochemical staining of Smad4 (**A**), Runx2 (**B**), tissue nonspecific alkaline phosphatase (TNAP) (**C**), osteopontin (OPN) (**D**), and bone sialoprotein (BSP) (**E**) in the apical root at P28. (**A,B**) Smad4- and Runx2-positive cells (arrows in **A,B**) are localized to the dental follicle at the root apex. (**C**) TNAP localization (asterisk) is detected at the periphery of the alveolar bone (AB). (**D,E**) OPN and BSP are localized to osteoblasts (arrows in **D,E**) and alveolar bone matrix. HRS, Hertwig's epithelial root sheath. Bar = 70 μm.

Literature Cited

Brock DP, Marty-Roix R, Spector M (2002) α-Smooth-muscle actin in and contraction of porcine dental pulp cells. J Dent Res 81: 203–208

Cai D, Marty-Roix R, Hsu HP, Spector M (2001) Lapine and canine bone marrow stromal cells contain smooth muscle actin and contract a collagen-glycosaminoglycan matrix. Tissue Eng 7:829–841

Chaponnier C, Gabbiani G (2004) Pathological situations characterized by altered actin isoform expression. J Pathol 204:386–395

Derynck R, Zhang Y, Feng XH (1998) Smads: transcriptional activators of TGF-beta responses. Cell 95:737–740

Hinz B, Dugina V, Ballestrem C, Wehrle-Haller B, Chaponnier C (2003) α-Smooth muscle actin is crucial for focal adhesion maturation in myofibroblasts. Mol Biol Cell 14:2508–2519

Hoshi K, Amizuka N, Oda K, Ikehara Y, Ozawa H (1997) Immunolocalization of tissue non-specific alkaline phosphatase in mice. Histochem Cell Biol 107:183–191

Hosoya A, Yoshiba K, Yoshiba N, Hoshi K, Iwaku M, Ozawa H (2003) An immunohistochemical study on hard tissue formation in a subcutaneously transplanted rat molar. Histochem Cell Biol 119:27–35

Kinner B, Zaleskas JM, Spector M (2002) Regulation of smooth muscle actin expression and contraction in adult human mesenchymal stem cells. Exp Cell Res 278:72–83

Kruzynska-Frejtag A, Wang J, Maeda M, Rogers R, Krug E, Hoffman S, Markwald RR, et al. (2004) Periostin is expressed within the developing teeth at the sites of epithelial-mesenchymal interaction. Dev Dyn 229:857–868

Lian JB, Javed A, Zaidi SK, Lengner C, Montecino M, van Wijnen AJ, Stein JL, et al. (2004) Regulatory controls for osteoblast growth and differentiation: role of Runx/Cbfa/AML factors. Crit Rev Eukaryot Gene Expr 14:1–48

Menard C, Mitchell S, Spector M (2000) Contractile behavior of smooth muscle actin-containing osteoblasts in collagen-GAG matrices in vitro: implant-related cell contraction. Biomaterials 21:1867–1877

Mukai K, Schollmeyer JV, Rosai J (1981) Immunohistochemical localization of actin: applications in surgical pathology. Am J Surg Pathol 5:91–97

Nanci A (2003) Ten Cate's Oral Histology: Development, Structure, and Function. 6th ed. St. Louis, Mosby 240–274

Saito M, Handa K, Kiyono T, Hattori S, Yokoi T, Tsubakimoto T, Harada H, et al. (2005) Immortalization of cementoblast progenitor cells with Bmi-1 and TERT. J Bone Miner Res 20:50–57

Schildmeyer LA, Braun R, Taffet G, Debiasi M, Burns AE, Bradley A, Schwartz RJ (2000) Impaired vascular contractility and blood pressure homeostasis in the smooth muscle α-actin null mouse. FASEB J 14:2213–2220

Schroeder HE (1991) Oral Structural Biology. New York, Thieme Medical Publishers, 4–37

Seo BM, Miura M, Gronthos S, Bartold PM, Batouli S, Brahim J, Young M, et al. (2004) Investigation of multipotent postnatal stem cells from human periodontal ligament. Lancet 364:149–155

Seo BM, Miura M, Sonoyama W, Coppe C, Stanyon R, Shi S (2005) Recovery of stem cells from cryopreserved periodontal ligament. J Dent Res 84:907–912

Shi Y, Massague J (2003) Mechanisms of TGF-beta signaling from cell membrane to the nucleus. Cell 113:685–700

Skalli O, Ropraz P, Trzeciak A, Benzonana G, Gillessen D, Gabbiani G (1986) A monoclonal antibody against alpha-smooth muscle actin: a new probe for smooth muscle differentiation. J Cell Biol 103:2787–2796

Suzuki H, Amizuka N, Kii I, Kawano Y, Nozawa-Inoue K, Suzuki A, Yoshie H, et al. (2004) Immunohistochemical localization of periostin in tooth and its surrounding tissues in mouse mandibles during development. Anat Rec A Discov Mol Cell Evol Biol 281:1264–1275

van Beurden HE, Von den Hoff JW, Torensma R, Maltha JC, Kuijpers-Jagtman AM (2005) Myofibroblasts in palatal wound healing: prospects for the reduction of wound contraction after cleft palate repair. J Dent Res 84:871–880

Yamada M, Kurihara H, Kinoshita K, Sakai T (2005) Temporal expression of alpha-smooth muscle actin and drebrin in septal interstitial cells during alveolar maturation. J Histochem Cytochem 53:735–744

Yamashiro T, Tummers M, Thesleff I (2003) Expression of bone morphogenetic proteins and Msx genes during root formation. J Dent Res 82:172–176